

Characterizing mixed state entanglement through single-photon interference

Mayukh Lahiri,^{1,*} Radek Lapkiewicz,² Armin Hochrainer,^{3,4} Gabriela Barreto Lemos,^{5,4,†} and Anton Zeilinger^{3,4,‡}

¹*Department of Physics, Oklahoma State University, Stillwater, Oklahoma, USA*

²*Institute of Experimental Physics, Faculty of Physics,
University of Warsaw, Pasteura 5, Warsaw 02-093, Poland*

³*Vienna Center for Quantum Science and Technology (VCQ), Faculty of Physics,
University of Vienna, Boltzmannngasse 5, Vienna A-1090, Austria.*

⁴*Institute for Quantum Optics and Quantum Information,
Austrian Academy of Sciences, Boltzmannngasse 3, Vienna A-1090, Austria.*

⁵*Physics Department, University of Massachusetts Boston,
100 Morrissey Boulevard, Boston MA 02125, USA.*

Entanglement verification and measurement is essential for experimental tests of quantum mechanics and also for quantum communication and information science. Standard methods of verifying entanglement in a bipartite mixed state require detection of both particles and involve coincidence measurement. We present a method that enables us to verify and measure entanglement in a two-photon mixed state without detecting one of the photons, i.e., without performing any coincidence measurement or postselection. We consider two identical sources, each of which can generate the same two-photon mixed state but they never emit simultaneously. We show that one can produce a set of single-photon interference patterns, which contain information about entanglement in the two-photon mixed state. We prove that it is possible to retrieve the information about entanglement from the visibility of the interference patterns. Our method reveals a distinct avenue for verifying and measuring entanglement in mixed states.

I. INTRODUCTION

Entanglement is a fascinating trait of quantum mechanics—in addition to its implications for the foundations of quantum mechanics, today entanglement is a key resource in quantum information science. Verification and measurement of entanglement in a quantum state is an ever growing field of research [1, 2]. Entanglement in two-particle (more generally bipartite) quantum states can be verified, for example, by the violation of Bell's inequalities [3–7], quantum state tomography [8], entanglement witnesses [9–14], and measurements employing multiple copies of the quantum state [15–20]. For a general bipartite quantum state, all these methods require detection of both particles (subsystems). Known methods of verifying entanglement by performing measurement on one subsystem require the bipartite state to be pure [21–24]. Whether the entanglement of a bipartite mixed state can be verified by detecting only one subsystem is a question of fundamental importance.

We show by an example that it is indeed possible to verify the entanglement in a two-particle mixed state without detecting one of the particles. No coincidence measurement or postselection is required in our method. In order to demonstrate our method, we choose a polarization entangled mixed state, which can be obtained by generalizing two Bell states. We use two identical sources of the quantum state but only one pair of photons is pro-

duced at a time, i.e., multiple copies of the state are *not* produced. We employ an interferometric technique to show that an entanglement criterion, namely the positive partial transpose criterion [25, 26], can be tested and the entanglement can also be measured by means of the concurrence, a popular measure of two-qubit entanglement [27, 28].

Here, we present a detailed theoretical analysis of the entanglement verification technique. Furthermore, the nonlinear interferometer [29–31] used in our scheme has recently found important applications to various branches of quantum science and technology, including quantum imaging [32, 33], quantum spectroscopy [34], polarization control [35], and fundamental test of quantum mechanics [36, 37]. All the corresponding theoretical analyses apply to pure states only. Our theoretical analysis also shows how to treat a mixed state in such an interferometric arrangement. The experimental results are included in a separate publication [38].

The article is organized as follows. In Sec. II we outline our entanglement analysis scheme. In Sec. III, we present the class of states we address and discuss the relevant entanglement criterion and measure. In Sec. IV, we present the analysis of our method and the main results, which also include illustrations by numerical examples. Finally, in Sec. V we summarize and present our conclusions.

II. OUTLINE OF THE SCHEME

We consider two identical sources, Q_1 and Q_2 , each of which can produce the same two-photon mixed state, $\hat{\rho}$; however, they never emit simultaneously (Fig. 1). We

*Electronic address: mlahiri@okstate.edu

†Electronic address: gabibl@if.ufrj.br

‡Electronic address: anton.zeilinger@univie.ac.at

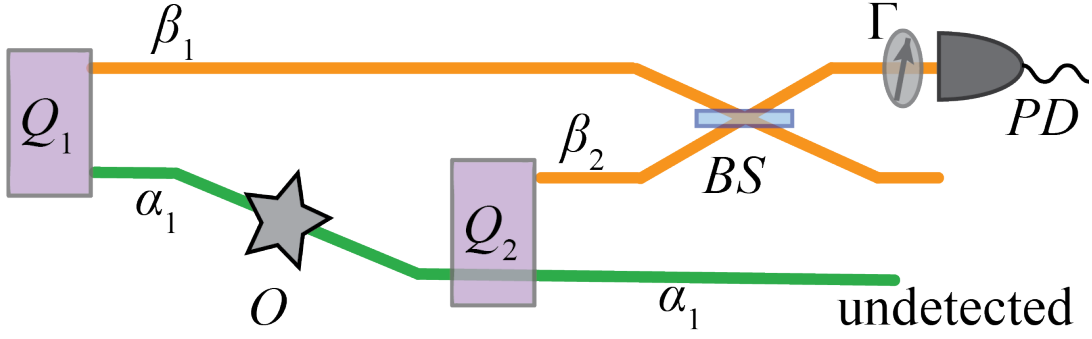


FIG. 1: Entanglement verification scheme. Two identical sources, Q_1 and Q_2 , individually generate the same two-photon state ($\hat{\rho}$). Source Q_1 can emit a photon pair (α, β) into propagation modes α_1 and β_1 . Source Q_2 is restricted to emit photon α also in the mode α_1 . Photon α , which is never detected, interacts with a device, O , between Q_1 and Q_2 . Source Q_2 can emit photon β in propagation mode β_2 . Modes β_1 and β_2 are combined by a beamsplitter (BS) and an output of BS is collected by a photo-detector (PD). Another device (Γ), placed before PD , allows us to choose the measurement basis. Sources Q_1 and Q_2 emit probabilistically and never emit simultaneously. When it is impossible to know the source of a detected photon, single-photon interference is observed at PD . For certain choices of basis, the entanglement of the two-photon state determines the visibility of the interference pattern. Information about the entanglement is retrieved from the single-photon interference patterns.

denote the two photons by α and β . Suppose that Q_1 can emit photon α into propagation mode α_1 . We ensure that Q_2 can emit photon α only in the same propagation mode (α_1). This is done by sending the beam of photon α generated by Q_1 through source Q_2 and perfectly aligning the beam with the beam of photon α generated by Q_2 . Therefore, if one only observes photon α that emerges from Q_2 , one cannot identify the origin of the photon.

Sources Q_1 and Q_1 can emit photon β into distinct propagation modes β_1 and β_2 , respectively. These two modes are superposed by a beam splitter, BS , and one of the outputs of BS is directed to a photon detector, PD . A device, Γ , is placed in front of PD to choose appropriate measurement bases. It is important to note that only the single-photon counting rate (intensity) is measured in the experiment and no coincidence measurement is ever performed.

A device, O , is placed in the path of photon α between Q_1 and Q_2 . (This device does not affect the emission rates at Q_1 and Q_2 .) Although α is never detected, the interaction with O affects the interference pattern recorded by detecting photon β at PD [29, 30]. This striking phenomenon forms the basis of our entanglement verification scheme. We show that with the knowledge of this interaction, the information about the entanglement in the two-photon quantum state can be retrieved from single-photon interference patterns recorded in certain measurement bases. It is evident that the choice of devices O and Γ depends on the entangled degree of freedom.

In order to illustrate the scheme we work with a two-photon polarization entangled state which is discussed in the next section.

III. THE QUANTUM STATE

We consider a two-photon polarization-entangled mixed state that can be characterized by three free parameters. Such a state can be expressed in the general form [49]

$$\hat{\rho} = I_H |H_\alpha, H_\beta\rangle \langle H_\alpha, H_\beta| + I_V |V_\alpha, V_\beta\rangle \langle V_\alpha, V_\beta| + (e^{-i\phi} \mathcal{I} \sqrt{I_H I_V} |H_\alpha, H_\beta\rangle \langle V_\alpha, V_\beta| + \text{H.c.}), \quad (1)$$

where $0 \leq I_H \leq 1$, $I_V = 1 - I_H$, ϕ is a phase, $0 \leq \mathcal{I} \leq 1$, and H and V represent horizontal and vertical directions of polarization respectively. It is evident that I_H , I_V , \mathcal{I} , and ϕ are all real quantities. When $\mathcal{I} = 1$, the density operator ($\hat{\rho}$) represents a pure state. When $\mathcal{I} = 0$ and $I_H = 1/2$ the state is diagonal in all bases, i.e. maximally mixed.

It is to be noted that $\hat{\rho}$ can be obtained by generalizing the two following Bell States: $|\Phi^+\rangle = (|H_\alpha, H_\beta\rangle + |V_\alpha, V_\beta\rangle)/\sqrt{2}$ and $|\Phi^-\rangle = (|H_\alpha, H_\beta\rangle - |V_\alpha, V_\beta\rangle)/\sqrt{2}$.

PPT Criterion.— Since we have a bipartite two dimensional entangled state, the criterion of positive partial transpose (PPT criterion) [25] can be applied to ensure separability or entanglement [26]. A partial transposition of two-particle density matrix ($\hat{\rho}$) is a transposition taken with respect to only one of the particles. The density operator $\hat{\rho}$ has a positive partial transpose if and only if its partial transposition does not have any negative eigenvalues. According to the PPT criterion, a bipartite two-dimensional state is separable if and only if $\hat{\rho}$ has positive partial transpose ([26], see also [1]).

We take the partial transposition of $\hat{\rho}$ [Eq. (1)] with respect to photon α and find that the resulting matrix has the following eigenvalues:

$$I_H, \quad I_V, \quad \mathcal{I} \sqrt{I_H I_V}, \quad -\mathcal{I} \sqrt{I_H I_V},$$

where $I_V = 1 - I_H$. Since \mathcal{J} , I_H , and I_V cannot take negative values, it follows from the PPT criterion that the state is entangled if and only if

$$\mathcal{J}\sqrt{I_H I_V} \neq 0. \quad (2)$$

Concurrence. — The amount of entanglement in the two-qubit state ($\hat{\rho}$) can be quantified by the concurrence [28]. In order to determine the concurrence one first needs to find the so-called “spin-flipped” density operator

$$\hat{\rho}^* = (\hat{\sigma}_y \otimes \hat{\sigma}_y) \hat{\rho}^* (\hat{\sigma}_y \otimes \hat{\sigma}_y), \quad (3)$$

where $\hat{\sigma}_y$ is the second Pauli operator, \otimes implies Kronecker product, and the asterisk (*) refers to the complex conjugation. The product $\hat{\rho}\hat{\rho}^*$ has only real and non-negative eigenvalues. If the square roots of these eigenvalues, in decreasing order, are λ_1 , λ_2 , λ_3 , and λ_4 , the concurrence of $\hat{\rho}$ is given by

$$\mathcal{C}(\hat{\rho}) = \max\{\lambda_1 - \lambda_2 - \lambda_3 - \lambda_4, 0\}. \quad (4)$$

It follows from Eqs. (1), (3), and (4) that in our case, the concurrence of the quantum state is

$$\mathcal{C}(\hat{\rho}) = 2\mathcal{J}\sqrt{I_H I_V} = 2\mathcal{J}\sqrt{I_H(1 - I_H)}. \quad (5)$$

Below we show that for the quantum state given by Eq. (1), the scheme allows us to test the PPT criterion as well as to measure the concurrence.

IV. ENTANGLEMENT VERIFICATION AND MEASUREMENT

A. Physical Realization

The quantum state under consideration is entangled in polarization. In this case, we choose the device O of Fig. 1 to be a half-wave plate (HWP). As for device Γ , we use a combination of wave plates and a polarizer such that photon β can be projected onto the horizontal (H), vertical (V), diagonal (D), anti-diagonal (A), right-circular (R) or left-circular (L) polarization state. The experimental setup is illustrated in Fig. 2.

Below we provide a detailed theoretical analysis explaining how the information about entanglement can be obtained from the single-photon interference patterns recorded at PD .

B. Deriving the Density Operator

For the convenience of analysis, we rewrite Eq. (1) in the following form:

$$\hat{\rho}_j = \sum_{\mu, \nu} \sqrt{I_\mu I_\nu} \mathcal{J}_{\mu\nu} \exp(i\phi_{\mu\nu}) |\mu_\alpha^j\rangle \langle \mu_\beta^j| \langle \nu_\alpha^j| \langle \nu_\beta^j|, \quad (6)$$

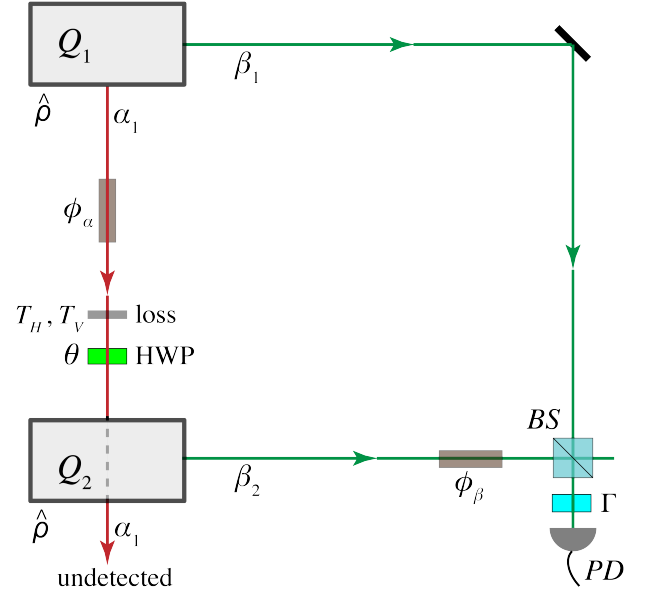


FIG. 2: Entanglement verification of a polarization-entangled state. Each source (Q_1 , Q_2) individually produces the state $\hat{\rho}$ [Eq. (1)]. Device O of Fig. 1 is now a half-wave plate (HWP) and device Γ projects photon β onto horizontal (H), vertical (V), diagonal (D), anti-diagonal (A), right-circular (R) or left-circular (L) polarization state. Photon β is detected at PD and photon α is not detected. For certain choices of HWP angle and certain choices of the measurement basis, the single-photon interference pattern recorded at PD contains information of entanglement in state $\hat{\rho}$.

where $j = 1, 2$ refers to the sources Q_1 and Q_2 ; $\mu = H, V$; $\nu = H, V$; $\phi_{\mu\nu} = 0$ for $\mu = \nu$, and $\phi_{HV} = -\phi_{VH} = -\phi$; and

$$\mathcal{J}_{\mu\nu} = \mathcal{J}_{\nu\mu} = \begin{cases} 1 & \text{for } \mu = \nu \\ \mathcal{J} & \text{for } \mu \neq \nu. \end{cases} \quad (7)$$

We recall that sources produce only one photon pair in one detection run. The most general state that such an arrangement can produce is given by (Appendix 1)

$$\hat{\rho}'_{\alpha\beta} = \sum_{j,k} \sum_{\mu,\nu}^{1,2} b_j b_k^* \sqrt{I_\mu I_\nu} P_{\mu^j}^{\nu^k} \exp(i\xi_{\mu^j}^{\nu^k}) |\mu_\alpha^j\rangle \langle \mu_\beta^j| \langle \nu_\alpha^k| \langle \nu_\beta^k|, \quad (8)$$

where both $j = 1, 2$ and $k = 1, 2$ refer to the sources, $|b_j|^2$ is the probability of the photon pair being emitted by source Q_j , $|b_1|^2 + |b_2|^2 = 1$; the asterisk (*) denotes complex conjugation, the phase $\xi_{\mu^j}^{\nu^k}$ and the real positive quantity $P_{\mu^j}^{\nu^k}$ must obey the relations (Appendix 1)

$$\xi_{\mu^j}^{\nu^k} = -\xi_{\nu^k}^{\mu^j} \quad \forall j, k, \mu, \nu, \quad \text{and} \quad \xi_{\mu^j}^{\nu^j} = \phi_{\mu\nu} \quad \forall j, \quad (9a)$$

$$P_{\mu^j}^{\nu^k} = P_{\nu^k}^{\mu^j} \quad \forall j, k, \mu, \nu, \quad \text{and} \quad P_{\mu^j}^{\nu^j} = \mathcal{J}_{\mu\nu} \quad \forall j, \quad (9b)$$

and $0 \leq P_{\mu^j}^{\nu^k} = P_{\nu^k}^{\mu^j} \leq 1$.

We now impose the condition that photon pairs emitted by separate sources are fully coherent when they have the same polarization, i.e.

$$P_{\mu^1}^{\mu^2} = P_{\mu^2}^{\mu^1} = 1 \quad \text{for } \mu = H, V. \quad (10)$$

This condition is easily attained in the laboratory by employing a pump laser with sufficiently long coherence length [38]. If we apply this condition, it follows from the positive semi-definiteness of $\hat{\rho}'_{\alpha\beta}$ that (Appendix 2)

$$P_{\mu^j}^{\nu^k} = \mathcal{J}_{\mu\nu}, \quad \forall j, k, \mu, \nu, \quad (11)$$

where $\mathcal{J}_{\mu\nu}$ is given by Eq. (7).

From Eqs. (8) and (11), we find that the density operator representing the state of a photon pair in our system is given by

$$\hat{\rho}_{\alpha\beta} = \sum_{j,k}^{1,2} \sum_{\mu,\nu} b_j b_k^* \sqrt{I_\mu I_\nu} \mathcal{J}_{\mu\nu} \exp(i\xi_{\mu^j}^{\nu^k}) |\mu_\alpha^j, \mu_\beta^j\rangle \langle \nu_\alpha^k, \nu_\beta^k|. \quad (12)$$

We now mathematically represent the interaction of HWP with photon α . Ideally, there should not be any loss of photon in the propagation mode α_1 between Q_1 and Q_2 . However, due to experimental imperfections it is almost impossible to avoid slight misalignment of paths and probabilistic absorption of photon α between Q_1 and Q_2 . In order to make our measurement scheme robust against such losses, we take them into account quantitatively. Let T_μ be the probability amplitude of photon α (polarized along direction μ) to arrive at Q_2 from Q_1 . Without any loss of generality, we can assume that T_μ is real and therefore $0 < T_\mu < 1$. The combined effect of HWP and the losses can be represented by the following relations involving field operators:

$$\hat{a}_{H_\alpha} = e^{i\phi_\alpha} [T_H(\hat{a}_{H_\alpha} \cos 2\theta + \hat{a}_{V_\alpha} \sin 2\theta) + R_H \hat{a}_{H_0}], \quad (13a)$$

$$\hat{a}_{V_\alpha} = e^{i\phi_\alpha} [T_V(\hat{a}_{H_\alpha} \sin 2\theta - \hat{a}_{V_\alpha} \cos 2\theta) + R_H \hat{a}_{V_0}], \quad (13b)$$

where \hat{a} represents photon annihilation operator: $\hat{a}_{\mu_\alpha}^\dagger |\text{vacuum}\rangle = |\mu_\alpha^j\rangle$ and \hat{a}_{μ_0} can be interpreted as the field of a lost photon; $R_\mu = \sqrt{1 - T_\mu^2}$; the HWP is set at angle θ ; and ϕ_α is the phase gained due to the propagation through air from Q_1 to Q_2 (assumed to be the same for all polarization directions).

We now proceed to derive the final form of the two-photon quantum state in the setup. Let us rewrite Eq. (13) in the compact form

$$\hat{a}_{\mu_\alpha} = e^{i\phi_\alpha} \left[\sum_{\lambda}^{H,V} \Lambda_{\mu\lambda}(\theta) \hat{a}_{\lambda_\alpha} + R_\mu \hat{a}_{\mu_0} \right], \quad \mu = H, V, \quad (14)$$

where $\Lambda_{HH}(\theta) = T_H \cos 2\theta$, $\Lambda_{HV}(\theta) = T_H \sin 2\theta$, $\Lambda_{VH}(\theta) = T_V \sin 2\theta$, and $\Lambda_{VV}(\theta) = -T_V \cos 2\theta$ are all real quantities. Using the facts that $\hat{a}_{\mu_\alpha}^\dagger |\text{vacuum}\rangle = |\mu_\alpha^j\rangle$ and $\hat{a}_{\mu_0}^\dagger |\text{vacuum}\rangle = |\mu\rangle_0$, we obtain from Eq. (14) the following transformation law for a ket:

$$|\mu_\alpha^2\rangle = e^{-i\phi_\alpha} \left[\sum_{\lambda}^{H,V} \Lambda_{\mu\lambda}(\theta) |\lambda_\alpha^1\rangle + R_\mu |\mu\rangle_0 \right], \quad (15)$$

where $\Lambda_{\mu\lambda}(\theta)$ is defined below Eq. (14). The final form of the density operator representing the two-photon quantum state is obtained by substituting Eq. (15) into Eq. (12). We denote this density operator by $\hat{\rho}_{\alpha\beta}^{(f)}$ and provide its explicit form in Appendix 3.

The density operator $\hat{\rho}_{\alpha\beta}^{(f)}$ (Appendix 3) can be used to determine the photon counting rate at the detector. Alternatively, one can also use the reduced density operator ($\hat{\rho}_\beta$), which represents the state of photon β only. We use the latter approach in our analysis. We obtain the reduced density operator ($\hat{\rho}_\beta$) by taking partial trace of $\hat{\rho}_{\alpha\beta}^{(f)}$ over the subspace of photon α and the loss modes. We find it to have the form

$$\begin{aligned} \hat{\rho}_\beta = & |b_1|^2 I_H |H_\beta\rangle \langle H_\beta| + |b_2|^2 I_H |H_\beta\rangle \langle H_\beta| \\ & + |b_1|^2 I_V |V_\beta\rangle \langle V_\beta| + |b_2|^2 I_V |V_\beta\rangle \langle V_\beta| \\ & + \left[b_1 b_2^* \cos 2\theta \left(I_H T_H \exp\{i(\phi_\alpha + \xi_{H_1}^{H_2})\} |H_\beta^1\rangle \langle H_\beta^2| \right. \right. \\ & \quad \left. \left. - I_V T_V \exp\{i(\phi_\alpha + \xi_{V_1}^{V_2})\} |V_\beta^1\rangle \langle V_\beta^2| \right) + \text{H.c.} \right] \\ & + \left[b_1 b_2^* \mathcal{J} \sqrt{I_H I_V} \sin 2\theta \left(T_V \exp\{i(\phi_\alpha + \xi_{H_1}^{V_2})\} |H_\beta^1\rangle \langle V_\beta^2| \right. \right. \\ & \quad \left. \left. + T_H \exp\{i(\phi_\alpha + \xi_{V_1}^{H_2})\} |V_\beta^1\rangle \langle H_\beta^2| \right) + \text{H.c.} \right]. \end{aligned} \quad (16)$$

C. Determining Photon Counting Rates and Visibility

We now show how to determine the single-photon counting rate. We recall that the propagation modes β_1 and β_2 are superposed by a beam splitter (BS) and one of the outputs of BS is sent through a device, Γ , which projects photon β onto a particular polarization state (H, V, D, A, R or L). Therefore, the positive-frequency part of the quantized electric field at the detector can be represented by

$$\hat{E}_{\mu_\beta}^{(+)} = \hat{a}_{\mu_\beta} + i e^{i\phi_\beta} \hat{a}_{\mu_\beta}^2, \quad \mu = H, V, D, A, R, L, \quad (17)$$

where $\hat{a}_{\mu_\beta}^j$ is the annihilation operator corresponding to photon β with polarization μ in beam β_j .

The single-photon counting rate (for a given polarization) at the detector can now be obtained by the standard formula

$$\mathcal{R}_\mu = \text{tr} \left\{ \hat{\rho}_\beta \hat{E}_{\mu_\beta}^{(-)} \hat{E}_{\mu_\beta}^{(+)} \right\}, \quad (18)$$

where $\hat{E}_{\mu\beta}^{(-)} = \{\hat{E}_{\mu\beta}^{(+)}\}^\dagger$; and $\hat{\rho}_\beta$ and $\hat{E}_{\mu\beta}^{(+)}$ are given by Eqs. (16) and (17) respectively. We show below in Sec. IV D that the photon counting rates measured for various polarizations represent various interference patterns. The visibility of such any such pattern is determined by the standard formula

$$\mathcal{V}_\mu = \frac{\mathcal{R}_\mu^{\max} - \mathcal{R}_\mu^{\min}}{\mathcal{R}_\mu^{\max} + \mathcal{R}_\mu^{\min}}, \quad (19)$$

where μ represents the polarization of the detected photon (β), and \mathcal{R}_μ^{\max} and \mathcal{R}_μ^{\min} are, respectively, the maximum and the minimum values of the single-photon counting rate.

In the next section (Sec. IV D), we show that the quantity $\mathcal{J}\sqrt{I_H I_V}$, which appears in the PPT-criterion [Eq. (2)] and also in the formula of concurrence [Eq. (5)], can be determined from the visibility of the above-mentioned single-photon interference patterns.

D. Signature of Entanglement in Single-photon Interference Patterns

We first consider the cases in which photon β is projected onto $|H_\beta\rangle$ and $|V_\beta\rangle$ polarization states. By the use of Eqs. (16), (17), and (18), we find that the photon counting rates are given by (we have applied $|b_1|^2 + |b_2|^2 = 1$)

$$\mathcal{R}_H = I_H \{1 + 2|b_1||b_2|T_H \cos 2\theta \sin(\phi_{in} + \xi_{H^1}^{H^2})\}, \quad (20a)$$

$$\mathcal{R}_V = I_V \{1 - 2|b_1||b_2|T_V \cos 2\theta \sin(\phi_{in} + \xi_{V^1}^{V^2})\}, \quad (20b)$$

where $\phi_{in} = \phi_\alpha - \phi_\beta + \arg\{b_1\} - \arg\{b_2\}$ is the interferometric phase that is modulated to obtain the interference patterns. It follows from Eqs. (19) and (20) that visibilities measured for H and V polarizations are

$$\mathcal{V}_H = 2|b_1||b_2|T_H \cos 2\theta, \quad (21a)$$

$$\mathcal{V}_V = 2|b_1||b_2|T_V \cos 2\theta. \quad (21b)$$

Clearly, when the half-wave plate is set at angle $\theta = 0$, the visibilities measured for these polarizations have their maximum values

$$\mathcal{V}_H|_{\theta=0} = 2|b_1||b_2|T_H; \quad \mathcal{V}_V|_{\theta=0} = 2|b_1||b_2|T_V. \quad (22)$$

We note that expressions of \mathcal{V}_H and \mathcal{V}_V do not contain I_H , I_V or \mathcal{J} . Therefore, measurement in this basis does not yield any information about entanglement. However, $\mathcal{V}_H|_{\theta=0}$ and $\mathcal{V}_V|_{\theta=0}$ provide us with a quantitative measure of the photon loss in the propagation mode α_1 . Therefore, it is crucial to measure them in an actual experiment.

We now consider the case when the polarization of the detected photon is diagonal (D), i.e., photon β is projected onto state $|D_\beta\rangle$ [50]. It follows from Eqs. (16),

(17), and (18) that the corresponding photon counting rate has the form

$$\begin{aligned} \mathcal{R}_D = \frac{1}{2} \bigg[& 1 + 2|b_1||b_2| \cos 2\theta \left\{ I_H T_H \sin(\phi_{in} + \xi_{H^1}^{H^2}) \right. \\ & \left. - I_V T_V \sin(\phi_{in} + \xi_{V^1}^{V^2}) \right\} \\ & + 2\mathcal{J}\sqrt{I_H I_V} |b_1||b_2| \sin 2\theta \left\{ T_V \sin(\phi_{in} + \xi_{V^1}^{V^2}) \right. \\ & \left. + T_H \sin(\phi_{in} + \xi_{H^1}^{H^2}) \right\} \bigg], \end{aligned} \quad (23)$$

where we have applied the formulas $|b_1|^2 + |b_2|^2 = 1$ and $I_H + I_V = 1$. We now set the half-wave plate angle to be $\pi/4$, i.e., $\cos 2\theta = 0$ and $\sin 2\theta = 1$. Under this condition Eq. (23) reduces to [51]

$$\begin{aligned} \mathcal{R}_D|_{\theta=\pi/4} = \frac{1}{2} \bigg[& 1 + 2\mathcal{J}\sqrt{I_H I_V} |b_1||b_2| \\ & \times \sqrt{T_H^2 + T_V^2 + 2T_H T_V \cos(\xi_{V^1}^{H^2} - \xi_{H^1}^{V^2})} \\ & \times \sin(\phi_{in} + \zeta) \bigg], \end{aligned} \quad (24)$$

where $\phi_{in} = \phi_\alpha - \phi_\beta + \arg\{b_1\} - \arg\{b_2\}$, and $\tan \zeta = T_H \sin(\xi_{V^1}^{H^2} - \xi_{H^1}^{V^2}) / [T_V + T_H \cos(\xi_{V^1}^{H^2} - \xi_{H^1}^{V^2})]$; the explicit form of ζ is not required for our purpose.

Following the same procedure, we find for $|A_\beta\rangle$ that the photon counting rate is given by [52]

$$\begin{aligned} \mathcal{R}_A|_{\theta=\pi/4} = \frac{1}{2} \bigg[& 1 - 2\mathcal{J}\sqrt{I_H I_V} |b_1||b_2| \\ & \times \sqrt{T_H^2 + T_V^2 + 2T_H T_V \cos(\xi_{V^1}^{H^2} - \xi_{H^1}^{V^2})} \\ & \times \sin(\phi_{in} + \zeta) \bigg]. \end{aligned} \quad (25)$$

It follows from Eqs. (19), (24), and (25) that the single-photon interference patterns recorded for D and A polarizations have the same visibility:

$$\begin{aligned} \mathcal{V}_D|_{\theta=\pi/4} = \mathcal{V}_A|_{\theta=\pi/4} = & 2\mathcal{J}\sqrt{I_H I_V} |b_1||b_2| \\ & \times \sqrt{T_H^2 + T_V^2 + 2T_H T_V \cos(\xi_{V^1}^{H^2} - \xi_{H^1}^{V^2})}. \end{aligned} \quad (26)$$

We note that the concurrence ($\mathcal{C}(\hat{\rho}) = 2\mathcal{J}\sqrt{I_H I_V}$) appears in the formulas of $\mathcal{V}_D|_{\theta=\pi/4}$ and $\mathcal{V}_A|_{\theta=\pi/4}$. This fact implies that the single-photon interference patterns recorded for diagonal and anti-diagonal polarizations contain information about the amount of entanglement in the two-photon mixed state.

Calculations for right-circular (R) and left-circular (L) polarizations are very similar to those for diagonal and anti-diagonal polarizations. When the half-wave plate angle is set such that $\theta = \pi/4$, the corresponding photon

counting rates become

$$\mathcal{R}_R|_{\theta=\frac{\pi}{4}} = \frac{1}{2} \left[1 - 2\mathcal{J}\sqrt{I_H I_V} |b_1| |b_2| \times \sqrt{T_H^2 + T_V^2 - 2T_H T_V \cos(\xi_{V1}^{H^2} - \xi_{H1}^{V^2})} \times \sin(\phi_{in} - \zeta') \right], \quad (27a)$$

$$\mathcal{R}_L|_{\theta=\frac{\pi}{4}} = \frac{1}{2} \left[1 + 2\mathcal{J}\sqrt{I_H I_V} |b_1| |b_2| \times \sqrt{T_H^2 + T_V^2 - 2T_H T_V \cos(\xi_{V1}^{H^2} - \xi_{H1}^{V^2})} \times \sin(\phi_{in} - \zeta') \right], \quad (27b)$$

where $\phi_{in} = \phi_\alpha - \phi_\beta + \arg\{b_1\} - \arg\{b_2\}$ and $\tan \zeta' = T_H \sin(\xi_{V1}^{H^2} - \xi_{H1}^{V^2}) / [T_V - T_H \cos(\xi_{V1}^{H^2} - \xi_{H1}^{V^2})]$; the explicit form of ζ' is not required for our purpose. Clearly, visibilities measured for R and L polarizations are given by

$$\mathcal{V}_R|_{\theta=\frac{\pi}{4}} = \mathcal{V}_L|_{\theta=\frac{\pi}{4}} = 2\mathcal{J}\sqrt{I_H I_V} |b_1| |b_2| \times \sqrt{T_H^2 + T_V^2 - 2T_H T_V \cos(\xi_{V1}^{H^2} - \xi_{H1}^{V^2})}. \quad (28)$$

The presence of the concurrence ($\mathcal{C}(\hat{\rho}) = 2\mathcal{J}\sqrt{I_H I_V}$) in Eqs. (27) and (28) shows that the single-photon interference patterns recorded for right-circular and left-circular polarizations contain information about the amount of entanglement in the two-photon mixed state.

We note that the visibilities measured for diagonal, anti-diagonal, right-circular, and left-circular polarizations are linearly proportional to the concurrence of the two-photon state ($\hat{\rho}$).

E. Test of the PPT Criterion

We now show that if $\mathcal{J}\sqrt{I_H I_V} \neq 0$, visibilities measured for diagonal (D) and right-circular (R) polarizations can never be simultaneously zero when the HWP-angle is set at $\theta = \pi/4$. It follows from Eqs. (26) and (28) that

$$\left(\mathcal{V}_D|_{\theta=\frac{\pi}{4}}\right)^2 + \left(\mathcal{V}_R|_{\theta=\frac{\pi}{4}}\right)^2 = 8|b_1|^2 |b_2|^2 (T_H^2 + T_V^2) \times (\mathcal{J}\sqrt{I_H I_V})^2. \quad (29)$$

Since $|b_1|$, $|b_2|$, T_H , and T_V must be non-zero quantities, $\mathcal{V}_D|_{\theta=\frac{\pi}{4}}$ and $\mathcal{V}_R|_{\theta=\frac{\pi}{4}}$ can be simultaneously equal to zero if and only if $\mathcal{J}\sqrt{I_H I_V} = 0$. According to the PPT criterion (Sec. III), the condition $\mathcal{J}\sqrt{I_H I_V} = 0$ implies that the two-photon mixed state [Eq. (1)] is separable. Since $\mathcal{V}_D|_{\theta=\frac{\pi}{4}} = \mathcal{V}_A|_{\theta=\frac{\pi}{4}}$ and $\mathcal{V}_R|_{\theta=\frac{\pi}{4}} = \mathcal{V}_L|_{\theta=\frac{\pi}{4}}$, it follows from the PPT criterion that when HWP is set at angle $\theta = \pi/4$, a non-zero value of the visibility (of the single-photon interference patterns) obtained for any one of polarizations D , A , R , and L confirms that the two-photon mixed state, $\hat{\rho}$ [Eq. (1)], is entangled. The

state is separable (not entangled) if and only if visibilities measured for *all of these polarizations* are zero.

We illustrate the test of PPT criterion by numerical examples in Sec. IV G.

F. Determining the Concurrence

It follows from the results of Sec. IV D that the concurrence, $\mathcal{C}(\hat{\rho})$, of the two-photon mixed state can be determined from the single-photon patterns. By the use of Eqs. (5), (22), and (29), we find that

$$\mathcal{C}(\hat{\rho}) = \sqrt{2 \frac{(\mathcal{V}_D|_{\theta=\frac{\pi}{4}})^2 + (\mathcal{V}_R|_{\theta=\frac{\pi}{4}})^2}{(\mathcal{V}_H|_{\theta=0})^2 + (\mathcal{V}_V|_{\theta=0})^2}}, \quad (30)$$

where D and R can be replaced by A and L respectively.

It follows from Eq. (30) that in order to determine the concurrence, one needs to measure visibilities not only for $|D_\beta\rangle$ (or $|A_\beta\rangle$) and $|R_\beta\rangle$ (or $|L_\beta\rangle$) but also for $|H_\beta\rangle$ and $|V_\beta\rangle$. However, we recall that although measurements corresponding to $|D_\beta\rangle$, $|A_\beta\rangle$, $|R_\beta\rangle$, or $|L_\beta\rangle$ yield information about entanglement, measurements corresponding to $|H_\beta\rangle$ and $|V_\beta\rangle$ do not. Therefore, it is natural to ask why measuring visibility for $|H_\beta\rangle$ and $|V_\beta\rangle$ is necessary to determine the concurrence.

Actually, under the ideal conditions ($|b_1| = |b_2| = 1/\sqrt{2}$ and $T_H = T_V = 1$), it is not required to measure the visibility for $|H_\beta\rangle$ and $|V_\beta\rangle$. It can be readily checked from Eq. (22) that in this case the denominator on the right hand side of Eq. (30) is equal to 1. However, no experimental situation is perfectly ideal. In particular, it is extremely challenging to achieve the condition $T_H = T_V = 1$ due to photon losses and imperfect alignment. Furthermore, emission probabilities at the two sources (Q_1 and Q_2) may not be equal, i.e., the condition $|b_1| = |b_2|$ may not always apply. The measurement of visibility when photon β is projected onto states $|H_\beta\rangle$ and $|V_\beta\rangle$ allows us to take care of these experimental imperfections. In fact, Eq. (30) shows that in spite of all such imperfections being present, one is able to determine the concurrence by the use of our method.

We present the experimentally measured values of concurrence of different mixed states in a separate publication [38]. Below we provide some numerical examples to illustrate our results.

G. Numerical Illustration of Results

We choose five density operators whose parameters are listed in Table I. We determine the values of concurrence of these states by the use of Eq. (5) and find that states $\hat{\rho}_1$ and $\hat{\rho}_2$ are separable, whereas state $\hat{\rho}_5$ is maximally entangled (a Bell state). Note that density operator $\hat{\rho}_1$ represents a pure state and $\hat{\rho}_2$ represents a fully mixed

state. States $\hat{\rho}_3$ and $\hat{\rho}_4$ are neither maximally entangled nor separable.

State	I_H	I_V	\mathcal{J}	Concurrence
$\hat{\rho}_1$	1	0	—	0
$\hat{\rho}_2$	0.5	0.5	0	0
$\hat{\rho}_3$	0.5	0.5	0.32	0.32
$\hat{\rho}_4$	0.5	0.5	0.5	0.5
$\hat{\rho}_5$	0.5	0.5	1	1

TABLE I: Two-photon mixed states used for illustration. The symbol “—” implies not applicable. Parameter ϕ [see Eq. (1)] is not displayed because it plays no role in determining the amount of entanglement.

For testing the PPT criterion with these states, we simulate an experimental situation in which experimental imperfections are present. In order to simulate the experimental imperfections, we assume that probabilities of emission at the two sources are not equal ($|b_1| \neq |b_2|$) and that there are photon losses in beam α_1 due to imperfect alignment ($T_H \neq 1$, $T_V \neq 1$). The parameters are chosen as follows: $|b_1|^2 = 0.55$, $|b_2|^2 = 0.45$, $T_H = 0.9$, $T_V = 0.85$, and $\xi_{V1}^{H^2} - \xi_{H1}^{V^2} = \pi/4$. By the use of Eqs. (26) and (28), we compute the visibility of the single-photon patterns recorded for $|D_\beta\rangle$, $|A_\beta\rangle$, $|R_\beta\rangle$, and $|L_\beta\rangle$. The values of visibility are listed in Table II.

State	$\mathcal{V}_D _{\theta=\pi/4}$	$\mathcal{V}_A _{\theta=\pi/4}$	$\mathcal{V}_R _{\theta=\pi/4}$	$\mathcal{V}_L _{\theta=\pi/4}$	PPT criterion
$\hat{\rho}_1$	0	0	0	0	separable
$\hat{\rho}_2$	0	0	0	0	separable
$\hat{\rho}_3$	0.76	0.76	0.31	0.31	entangled
$\hat{\rho}_4$	0.40	0.40	0.17	0.17	entangled
$\hat{\rho}_5$	0.80	0.80	0.33	0.33	entangled

TABLE II: Test of the PPT criterion for five different two-photon mixed states (Table I). Choice of parameters: $|b_1|^2 = 0.55$, $|b_2|^2 = 0.45$, $T_H = 0.9$, $T_V = 0.85$, and $\xi_{V1}^{H^2} - \xi_{H1}^{V^2} = \pi/4$. For separable (not-entangled) states, visibilities measured for $|D_\beta\rangle$, $|A_\beta\rangle$, $|R_\beta\rangle$, or $|L_\beta\rangle$ are all zero.

We find that for separable states ($\hat{\rho}_1$ and $\hat{\rho}_2$) the visibilities obtained for $|D_\beta\rangle$, $|A_\beta\rangle$, $|R_\beta\rangle$, and $|L_\beta\rangle$ are all equal to zero. Non-zero values of visibility for one of these polarizations confirm entanglement in the two-photon state.

We now illustrate how the concurrence of the two-photon mixed state can be determined from the single-photon interference patterns even when experimental imperfections are present. For simplicity of notation, we denote the quantity $\sqrt{(\mathcal{V}_D|_{\theta=\pi/4})^2 + (\mathcal{V}_R|_{\theta=\pi/4})^2}$ by S and the quantity $\sqrt{[(\mathcal{V}_H|_{\theta=0})^2 + (\mathcal{V}_V|_{\theta=0})^2]/2}$ by N . In this notation, the right hand side of Eq. (30) becomes S/N .

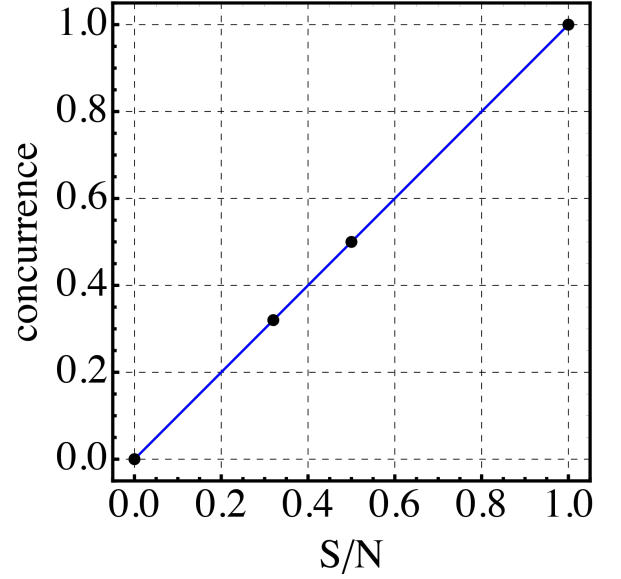


FIG. 3: Determining Concurrence from single-photon visibility. Experimental imperfections are simulated by choosing $|b_1|^2 = 0.55$, $|b_2|^2 = 0.45$, $T_H = 0.9$, and $T_V = 0.85$. Simulated data points (filled circles) represent computed values of the concurrence and of S/N for five quantum states given by Table I. (Data points for $\hat{\rho}_1$ and $\hat{\rho}_2$ coincide.) All simulated data points lie on the straight line predicted by Eq. (30) showing that the concurrence is equal to S/N despite the presence of experimental imperfections.

We choose the same experimental parameters given above. For the five states given by Table I, we compute the values of the concurrence in two ways: i) by the use of Eq. (5); and ii) by determining the values of S and N from Eqs. (22), (26), and (28). In Fig. 3, we plot the obtained values of the concurrence against S/N and find that they lie exactly on the straight line predicted by Eq. (30). Since both S and N can be measured experimentally, Fig. 3 illustrates that the concurrence of a two-photon mixed state can be experimentally determined from single-photon interference patterns.

V. SUMMARY AND CONCLUSIONS

We have shown that it is possible to verify and measure entanglement in a two-particle mixed state without detecting one of the particles and without any postselection.

To demonstrate our method, we have chosen a mixed state that can be obtained by generalizing two Bell states (see Sec. III). It is straightforward to show that our method also applies to the mixed state which can be obtained by generalizing the other two Bell states [53]. Therefore, our method currently covers all four Bell states and any two-dimensional mixed state that is ob-

tained by generalizing them.

Our method is based on the concept of path identity [29, 30]. This concept has recently drawn considerable attention after it has found important applications to imaging [32, 33], spectroscopy [34], microwave superconducting cavities [39], polarization control [35], optical coherence tomography [40, 41], the measurement of momentum correlation [42, 43], the generation of entangled states [44–48], and fundamental test of quantum mechanics [36, 37]. Like many of these applications, our entanglement verification method requires detection of only one of the particles of a two-particle system. Therefore, our method will be practically useful to test entanglement of a two-particle mixed state when a detector for one of the particles is not available.

Finally, our results open up a distinct avenue in verifying and measuring entanglement. They also inspire further questions. For example, one may now ask how to generalize the method so that it applies to many-particle high-dimensional entangled states.

VI. ACKNOWLEDGEMENTS

We acknowledge support from the Austrian Academy of Sciences (ÖAW- 462 IQOQI, Vienna) and the Austrian Science Fund (FWF) with SFB F40 (FOQUS) and W1210-2 (CoQus). M.L. also acknowledges support from the College of Arts and Sciences and the Office of the Vice President for Research, Oklahoma State University. R.L. was supported by the National Science Centre (Poland) grants 2015/17/D/ST2/03471, 2015/16/S/ST2/00424, the Polish Ministry of Science and Higher Education, and the Foundation for Polish Science (FNP) under the FIRST TEAM project “Spatiotemporal photon correlation measurements for quantum metrology and super-resolution microscopy” cofinanced by the European Union under the European Regional Development Fund.

Appendix 1: Density operator represented by Eqs. (8) and (9)

Here, we derive the density operator given by Eqs. (8) and (9).

In order to derive the density operator, we first recall two important facts: 1) the sources Q_1 and Q_2 emit in such a way that they jointly produce only one photon pair at a time, i.e., the density operator must represent a state that is occupied by only two photons; and 2) the sources cannot produce biphoton states of the form $|H_\alpha, V_\beta\rangle$ and $|V_\alpha, H_\beta\rangle$. Therefore, the most general form

that the density operator can take is given by

$$\hat{\rho}'_{\alpha\beta} = \sum_{j,k} \sum_{\mu,\nu}^{1,2} b_j b_k^* \sqrt{I_\mu^j I_\nu^k} P_{\mu^j}^{\nu^k} \exp(i\xi_{\mu^j}^{\nu^k}) |\mu_\alpha^j, \mu_\beta^j\rangle \langle \nu_\alpha^k, \nu_\beta^k|, \quad (\text{A-31})$$

where $j = 1, 2$ and $k = 1, 2$ represent the sources; $\mu = H, V$ and $\nu = H, V$; $|b_j|^2$ is the probability of the photon pair being emitted by source Q_j ; $|b_1|^2 + |b_2|^2 = 1$; I_μ^j is the probability with which source Q_j emits the photon pair $|\mu_\alpha, \mu_\beta\rangle$; $P_{\mu^j}^{\nu^k}$ is a non-negative real quantity; and $\xi_{\mu^j}^{\nu^k}$ is a phase (real quantity). Since Q_1 and Q_2 are identical sources, I_μ^j does not depend of j ; we therefore drop this superscript and obtain the form (Eq. (8) in main text)

$$\hat{\rho}'_{\alpha\beta} = \sum_{j,k} \sum_{\mu,\nu}^{1,2} b_j b_k^* \sqrt{I_\mu I_\nu} P_{\mu^j}^{\nu^k} \exp(i\xi_{\mu^j}^{\nu^k}) |\mu_\alpha^j, \mu_\beta^j\rangle \langle \nu_\alpha^k, \nu_\beta^k|, \quad (\text{A-32})$$

One can readily check that this density operator has unit trace. Below we derive the conditions that the coefficients associated with the density operator must obey.

If Q_2 does not emit (i.e., $|b_2| = 0$ and $|b_1| = 1$), the density operator, $\hat{\rho}'_{\alpha\beta}$, must reduce to the state of light generated by Q_1 alone (i.e., state $\hat{\rho}_1$ given by Eq. (6)). Likewise, if Q_1 does not emit (i.e., $|b_1| = 0$ and $|b_2| = 1$), the density operator, $\hat{\rho}'_{\alpha\beta}$, must reduce to the state of light generated by Q_2 alone (i.e., state $\hat{\rho}_2$ given by Eq. (6)). Using these two facts, we immediately obtain

$$\xi_{\mu^j}^{\nu^j} = \phi_{\mu\nu}, \quad \text{and} \quad P_{\mu^j}^{\nu^j} = \mathcal{J}_{\mu\nu}; \quad j = 1, 2. \quad (\text{A-33})$$

Furthermore, the density operator must be Hermitian. We therefore have

$$\xi_{\mu^j}^{\nu^k} = -\xi_{\nu^k}^{\mu^j}, \quad \text{and} \quad P_{\mu^j}^{\nu^k} = P_{\nu^k}^{\mu^j}; \quad \forall j, k, \mu, \nu. \quad (\text{A-34})$$

This completes the derivation of the density operator given by Eqs. (8) and (9).

Appendix 2: Derivation of Eq. (11)

In this appendix, we derive Eq. (11) by the use of Eqs. (8), (9), and (10). Eqs. (8) and (9) has already been redisplayed in Appendix 1. For the convenience of readers we display Eq. (10) once again below:

$$P_{\mu^1}^{\mu^2} = P_{\mu^2}^{\mu^1} = 1 \quad \text{for} \quad \mu = H, V. \quad (\text{A-35})$$

We note that the matrix elements of the density operator [Eq. (8)] contain four kinds of parameters: b_j , I_μ , $P_{\mu^j}^{\nu^k}$, and $\xi_{\mu^j}^{\nu^k}$. Each of them has a distinct physical meaning, and their values do *not* depend on each other. For example, the value of $P_{\mu^j}^{\nu^k}$ does not change if the values of b_j , I_μ , and $\xi_{\mu^j}^{\nu^k}$ are changed. This fact allows for a very

simple derivation of Eq. (11). We set $b_1 = b_2 = 1/\sqrt{2}$, $I_H = I_V = 1/2$, and $\xi_{\mu j}^{\nu k} = 0$ and represent the density operator in the following matrix form by combining Eqs. (8), (9), and (10):

$$\begin{pmatrix} \frac{1}{4} & 0 & 0 & \frac{\mathcal{J}}{4} & \frac{1}{4} & 0 & 0 & \frac{P_{H1}^{V2}}{4} \\ 0 & 0 & 0 & 0 & 0 & 0 & 0 & 0 \\ 0 & 0 & 0 & 0 & 0 & 0 & 0 & 0 \\ \frac{\mathcal{J}}{4} & 0 & 0 & \frac{1}{4} & \frac{P_{V1}^{H2}}{4} & 0 & 0 & \frac{1}{4} \\ \frac{1}{4} & 0 & 0 & \frac{P_{V1}^{H2}}{4} & \frac{1}{4} & 0 & 0 & \frac{\mathcal{J}}{4} \\ 0 & 0 & 0 & 0 & 0 & 0 & 0 & 0 \\ 0 & 0 & 0 & 0 & 0 & 0 & 0 & 0 \\ \frac{P_{H1}^{V2}}{4} & 0 & 0 & \frac{1}{4} & \frac{\mathcal{J}}{4} & 0 & 0 & \frac{1}{4} \end{pmatrix}. \quad (\text{A-36})$$

Since a density matrix must be positive semi-definite, the real symmetric matrix given by Eq. (A-36) must have nonnegative eigenvalues. The characteristic equation of this matrix can be expressed in the following form:

$$x^8 - x^7 + c_2 x^6 - c_3 x^5 + c_4 x^4 = 0, \quad (\text{A-37})$$

the coefficients c_2 , c_3 , and c_4 are real numbers and the so-

lutions of this equation are the eigenvalues of the matrix. All solutions of the characteristic equations are nonnegative when $c_j \geq 0$ for $j = 2, 3, 4$. From the relation $c_3 \geq 0$, we obtain

$$\left(P_{H1}^{V2} - \mathcal{J}\right)^2 + \left(P_{V1}^{H2} - \mathcal{J}\right)^2 \leq 0. \quad (\text{A-38})$$

Since the quantity on the left hand side of this inequality cannot take negative values, we must have

$$P_{H1}^{V2} = P_{V1}^{H2} = \mathcal{J}. \quad (\text{A-39})$$

This relationships given by Eqs. (10), (9b), and (A-39) are jointly represented by Eq. (11):

$$P_{\mu j}^{\nu k} = \mathcal{J}_{\mu\nu}, \quad \forall j, k, \mu, \nu. \quad (\text{A-40})$$

Appendix 3: Explicit Form of the Final Density Operator

Here we provide the explicit form of the density operator, $\hat{\rho}_{\alpha\beta}^{(f)}$, representing the photon pair in our system. We substitute Eq. (15) into Eq. (12) and find that

$$\begin{aligned} \hat{\rho}_{\alpha\beta}^{(f)} = & \sum_{\mu,\nu}^{H,V} |b_1|^2 \sqrt{I_\mu I_\nu} \mathcal{J}_{\mu\nu} \exp(i\phi_{\mu\nu}) |\mu_\alpha^1, \mu_\beta^1\rangle \langle \nu_\alpha^1, \nu_\beta^1| + \sum_{\mu,\nu}^{H,V} b_1 b_2^* \sqrt{I_\mu I_\nu} \mathcal{J}_{\mu\nu} \exp[i(\xi_{\mu 1}^{\nu 2} + \phi_\alpha)] R_\nu |\mu_\alpha^1, \mu_\beta^1\rangle \langle \nu_0, \nu_\beta^2| \\ & + \sum_{\mu,\nu}^{H,V} b_1^* b_2 \sqrt{I_\mu I_\nu} \mathcal{J}_{\mu\nu} \exp[i(\xi_{\mu 2}^{\nu 1} - \phi_\alpha)] R_\mu |\mu_0, \mu_\beta^2\rangle \langle \nu_\alpha^1, \nu_\beta^1| \\ & + \sum_{\mu,\nu}^{H,V} |b_2|^2 \sqrt{I_\mu I_\nu} \mathcal{J}_{\mu\nu} \exp(i\phi_{\mu\nu}) \left[R_\mu R_\nu |\mu_0, \mu_\beta^2\rangle \langle \nu_0, \nu_\beta^2| + R_\nu \sum_{\lambda}^{H,V} \Lambda_{\mu\lambda}(\theta) |\lambda_\alpha^1, \mu_\beta^2\rangle \langle \nu_0, \nu_\beta^2| \right. \\ & \left. + R_\mu \sum_{\lambda}^{H,V} \Lambda_{\nu\lambda}(\theta) |\mu_0, \mu_\beta^2\rangle \langle \lambda_\alpha^1, \nu_\beta^2| + \sum_{\lambda}^{H,V} \sum_{\epsilon}^{H,V} \Lambda_{\mu\lambda}(\theta) \Lambda_{\nu\epsilon}(\theta) |\lambda_\alpha^1, \mu_\beta^2\rangle \langle \epsilon_\alpha^1, \nu_\beta^2| \right]. \end{aligned} \quad (\text{A-41})$$

-
- [1] O. Ghne and G. Tth, Physics Reports **474**, 1 (2009), ISSN 0370-1573, URL <http://www.sciencedirect.com/science/article/pii/S0370157309000623>.
 - [2] R. Horodecki, P. Horodecki, M. Horodecki, and K. Horodecki, Rev. Mod. Phys. **81**, 865 (2009), URL <https://link.aps.org/doi/10.1103/RevModPhys.81.865>.
 - [3] J. S. Bell, Physics **1**, 195 (1964).
 - [4] J. F. Clauser, M. A. Horne, A. Shimony, and R. A. Holt, Phys. Rev. Lett. **23**, 880 (1969).
 - [5] S. J. Freedman and J. F. Clauser, Phys. Rev. Lett. **28**, 938 (1972), URL <https://link.aps.org/doi/10.1103/PhysRevLett.28.938>.
 - [6] A. Aspect, P. Grangier, and G. Roger, Phys. Rev. Lett. **49**, 91 (1982), URL <https://link.aps.org/doi/10.1103/PhysRevLett.49.91>.
 - [7] M. Giustina, M. A. M. Versteegh, S. Wengerowsky, J. Handsteiner, A. Hochrainer, K. Phelan, F. Steinlechner, J. Kofler, J.-A. Larsson, C. Abelln, et al., Phys. Rev. Lett. **115**, 250401 (2015), URL <https://link.aps.org/doi/10.1103/PhysRevLett.115.250401>.
 - [8] D. F. V. James, P. G. Kwiat, W. J. Munro, and A. G. White, Phys. Rev. A **64**, 052312 (2001), URL <https://link.aps.org/doi/10.1103/PhysRevA.64.052312>.
 - [9] O. Ghne, P. Hyllus, D. Bru, A. Ekert, M. Lewenstein, C. Macchiavello, and A. Sanpera, Phys. Rev. A

- 66, 062305 (2002), URL <https://link.aps.org/doi/10.1103/PhysRevA.66.062305>.
- [10] M. Barbieri, F. De Martini, G. Di Nepi, P. Mataloni, G. M. D'Ariano, and C. Macchiavello, Phys. Rev. Lett. **91**, 227901 (2003), URL <https://link.aps.org/doi/10.1103/PhysRevLett.91.227901>.
- [11] R. A. Bertlmann, K. Durstberger, B. C. Hiesmayr, and P. Krammer, Phys. Rev. A **72**, 052331 (2005), URL <https://link.aps.org/doi/10.1103/PhysRevA.72.052331>.
- [12] H. S. Park, S.-S. B. Lee, H. Kim, S.-K. Choi, and H.-S. Sim, Phys. Rev. Lett. **105**, 230404 (2010), URL <https://link.aps.org/doi/10.1103/PhysRevLett.105.230404>.
- [13] J. Dai, Y. L. Len, Y. S. Teo, B.-G. Englert, and L. A. Krivitsky, Phys. Rev. Lett. **113**, 170402 (2014), URL <https://link.aps.org/doi/10.1103/PhysRevLett.113.170402>.
- [14] K. Bartkiewicz, P. Horodecki, K. Lemr, A. Miranowicz, and K. Życzkowski, Phys. Rev. A **91**, 032315 (2015), URL <https://link.aps.org/doi/10.1103/PhysRevA.91.032315>.
- [15] P. Horodecki, Phys. Rev. Lett. **90**, 167901 (2003), URL <https://link.aps.org/doi/10.1103/PhysRevLett.90.167901>.
- [16] C. Schmid, N. Kiesel, W. Wiecek, H. Weinfurter, F. Mintert, and A. Buchleitner, Phys. Rev. Lett. **101**, 260505 (2008), URL <https://link.aps.org/doi/10.1103/PhysRevLett.101.260505>.
- [17] F. Mintert and A. Buchleitner, Phys. Rev. Lett. **98**, 140505 (2007), URL <https://link.aps.org/doi/10.1103/PhysRevLett.98.140505>.
- [18] C. Zhang, S. Yu, Q. Chen, and C. H. Oh, Phys. Rev. A **84**, 052112 (2011), URL <https://link.aps.org/doi/10.1103/PhysRevA.84.052112>.
- [19] L.-H. Zhang, Q. Yang, M. Yang, W. Song, and Z.-L. Cao, Phys. Rev. A **88**, 062342 (2013).
- [20] R. Islam, R. Ma, P. M. Preiss, M. E. Tai, A. Lukin, M. Rispoli, and M. Greiner, Nature **528**, 77 (2015).
- [21] S. Walborn, P. S. Ribeiro, L. Davidovich, F. Mintert, and A. Buchleitner, Nature **440**, 1022 (2006).
- [22] H. Di Lorenzo Pires, C. H. Monken, and M. P. van Exter, Phys. Rev. A **80**, 022307 (2009), URL <https://link.aps.org/doi/10.1103/PhysRevA.80.022307>.
- [23] F. Just, A. Cavanna, M. V. Chekhova, and G. Leuchs, New Journal of Physics **15**, 083015 (2013).
- [24] P. Sharapova, A. M. Pérez, O. V. Tikhonova, and M. V. Chekhova, Phys. Rev. A **91**, 043816 (2015), URL <https://link.aps.org/doi/10.1103/PhysRevA.91.043816>.
- [25] A. Peres, Phys. Rev. Lett. **77**, 1413 (1996), URL <https://link.aps.org/doi/10.1103/PhysRevLett.77.1413>.
- [26] P. Horodecki, Physics Letters A **232**, 333 (1997), ISSN 0375-9601, URL <http://www.sciencedirect.com/science/article/pii/S0375960197004167>.
- [27] S. Hill and W. K. Wootters, Phys. Rev. Lett. **78**, 5022 (1997).
- [28] W. K. Wootters, Phys. Rev. Lett. **80**, 2245 (1998).
- [29] X. Y. Zou, L. J. Wang, and L. Mandel, Phys. Rev. Lett. **67**, 318 (1991), URL <https://link.aps.org/doi/10.1103/PhysRevLett.67.318>.
- [30] L. J. Wang, X. Y. Zou, and L. Mandel, Phys. Rev. A **44**, 4614 (1991), URL <https://link.aps.org/doi/10.1103/PhysRevA.44.4614>.
- [31] M. Chekhova and Z. Ou, Advances in Optics and Photonics **8**, 104 (2016).
- [32] G. B. Lemos, V. Borish, G. D. Cole, S. Ramelow, R. Lapkiewicz, and A. Zeilinger, Nature **512**, 409 (2014).
- [33] M. Lahiri, R. Lapkiewicz, G. B. Lemos, and A. Zeilinger, Phys. Rev. A **92**, 013832 (2015).
- [34] D. A. Kalashnikov, A. V. Paterova, S. P. Kulik, and L. A. Krivitsky, Nature Photonics **10**, 98 (2016).
- [35] M. Lahiri, A. Hochrainer, R. Lapkiewicz, G. B. Lemos, and A. Zeilinger, Phys. Rev. A **95**, 033816 (2017), URL <https://link.aps.org/doi/10.1103/PhysRevA.95.033816>.
- [36] A. Heuer, R. Menzel, and P. W. Milonni, Phys. Rev. Lett. **114**, 053601 (2015), URL <https://link.aps.org/doi/10.1103/PhysRevLett.114.053601>.
- [37] A. Heuer, R. Menzel, and P. W. Milonni, Phys. Rev. A **92**, 033834 (2015), URL <https://link.aps.org/doi/10.1103/PhysRevA.92.033834>.
- [38] G. B. Lemos, R. Lapkiewicz, A. Hochrainer, M. Lahiri, and A. Zeilinger, submitted to Phys. Rev. Lett. (2019).
- [39] P. Lähteenmäki, G. S. Paraoanu, J. Hassel, and P. J. Hakonen, Nature communications **7**, 1 (2016).
- [40] A. Vallés, G. Jiménez, L. J. Salazar-Serrano, and J. P. Torres, Phys. Rev. A **97**, 023824 (2018).
- [41] A. V. Paterova, H. Yang, C. An, D. A. Kalashnikov, and L. A. Krivitsky, Quantum Science and Technology **3**, 025008 (2018), URL <https://doi.org/10.1088/2F2058-9565/2Faab567>.
- [42] M. Lahiri, A. Hochrainer, R. Lapkiewicz, G. B. Lemos, and A. Zeilinger, Phys. Rev. A **96**, 013822 (2017).
- [43] A. Hochrainer, M. Lahiri, R. Lapkiewicz, G. B. Lemos, and A. Zeilinger, Proceedings of the National Academy of Sciences **114**, 1508 (2017).
- [44] M. Lahiri, Phys. Rev. A **98**, 033822 (2018), URL <https://link.aps.org/doi/10.1103/PhysRevA.98.033822>.
- [45] M. Krenn, A. Hochrainer, M. Lahiri, and A. Zeilinger, Phys. Rev. Lett. **118**, 080401 (2017), URL <https://link.aps.org/doi/10.1103/PhysRevLett.118.080401>.
- [46] J. Kysela, M. Erhard, A. Hochrainer, M. Krenn, and A. Zeilinger, arXiv preprint arXiv:1904.07851 (2019).
- [47] D. E. Bruschi, C. Sabín, and G. S. Paraoanu, Phys. Rev. A **95**, 062324 (2017), URL <https://link.aps.org/doi/10.1103/PhysRevA.95.062324>.
- [48] G. Zhang, C. Bian, L. Chen, Z. Ou, and W. Zhang, New Journal of Physics **14**, 063034 (2012).
- [49] It is important to note that our entanglement verification scheme can also be applied to states $\hat{\rho} = I_1|H_\alpha V_\beta\rangle\langle H_\alpha V_\beta| + I_2|V_\alpha H_\beta\rangle\langle V_\alpha H_\beta| + (\mathcal{J}\sqrt{I_1 I_2}e^{-i\phi}|H_\alpha V_\beta\rangle\langle V_\alpha H_\beta| + \text{H.c.})$.
- [50] Note that $|D\rangle = (|H\rangle + |V\rangle)/\sqrt{2}$.
- [51] We have applied the trigonometric identity $p\sin x + q\sin(x + \delta) = \sqrt{p^2 + q^2 + 2pq\cos\delta}\sin(x + \zeta'')$, where $\tan\zeta'' = q\sin\delta/(p + q\cos\delta)$.
- [52] Note that $|A\rangle = (|V\rangle - |H\rangle)/\sqrt{2}$.
- [53] This mixed state has the form $\hat{\rho} = I_1|H_\alpha, V_\beta\rangle\langle H_\alpha, V_\beta| + I_2|V_\alpha, H_\beta\rangle\langle V_\alpha, H_\beta| + (e^{-i\phi}\mathcal{J}\sqrt{I_1 I_2}|H_\alpha, V_\beta\rangle\langle V_\alpha, H_\beta| + \text{H.c.})$. It is obtained by generalizing the two Bell states $|\Psi^+\rangle = (|H_\alpha, V_\beta\rangle + |V_\alpha, H_\beta\rangle)/\sqrt{2}$ and $|\Psi^-\rangle = (|H_\alpha, V_\beta\rangle - |V_\alpha, H_\beta\rangle)/\sqrt{2}$.